

Affine Invariant Erosion of 3D Shapes

Santiago Betelu

Institute for Mathematics and its Applications
Minneapolis, MN 55455
betelu@ima.umn.edu

Guillermo Sapiro

Department of Electrical and Computer Engineering
University of Minnesota, Minneapolis, MN 55455
guille@mail.ece.umn.edu

Allen Tannenbaum

School of Electrical and Computer Engineering
Georgia Institute of Technology Atlanta, GA 30322-0535
tannenba@ece.gatech.edu

Abstract

A new definition of affine invariant erosion of 3D surfaces is introduced. Instead of being based in terms of Euclidean distances, the volumes enclosed between the surface and its chords are used. The resulting erosion is insensitive to noise, and by construction, it is affine invariant. We prove some key properties about this erosion operation, and we propose a simple method to compute the erosion of implicit surfaces. We also discuss how the affine erosion can be used to define 3D affine invariant robust skeletons.

1. Introduction

This work deals with a new definition of affine erosion of 3D shapes. Erosion is a fundamental operation in mathematical morphology and shape analysis in general (e.g., for the computation of skeletons and general filters following Matheron's representation theorem). In the classical 2D definition [8, 19, 15, 7], the erosion $e_r(V)$ of a set V is computed as

$$e_r(V) = V \ominus B = \{x : B_x \subset V\},$$

where B is the *structuring element*, \ominus is the Minkowski subtraction, and B_x denotes the translation of B so that its origin is located at x . In the isotropic case, B is a circle of radius r . The extension to three dimensions is straightforward, using a sphere instead of a circle. In a different def-

inition, the erosion $e_r(V)$ is the shape that results by propagating a distance r the boundary ∂V of V in the direction of its inwards normal N . This is equivalent to thresholding the distance function [18].

This operation is often used in combination with other morphological operations in order to perform different tasks, as for example, to morphologically smooth out noisy data and to compute skeletons.

Here, we construct a different definition of erosion $\Gamma_v(V)$ which is invariant under the *special affine transformation*

$$\mathbf{X}' = \mathbf{A} \cdot \mathbf{X} + \mathbf{T}, \quad (1)$$

where \mathbf{X} , \mathbf{X}' and \mathbf{T} are vectors in \mathbf{R}^3 and \mathbf{A} is a 3×3 matrix of determinant equal to one. By *affine invariant* we mean that if the points on the volume V are transformed by Eq. (1), then the erosion $\Gamma_v(V)$ will be transformed in the same way. The parameter v , which has dimensions of volume, plays the same role of r in the Euclidean erosion. For the two-dimensional case, the affine erosion was studied in [12, 13], and then used and extended in [1] to compute affine invariant skeletons.

Here we make an extension to three dimensions, and define the erosion in terms of the volumes enclosed between the surface and its chords. We use chordal volumes because they are invariant with respect to Eq. (1). First we construct an *affine erosion level-set function* $E(\mathbf{x}, V)$ as the absolute minimum of the volumes of the chordal sets containing \mathbf{x} , and then the *erosion-sets* as the points enclosed by the contour surfaces of $E(\mathbf{x}, V)$. The erosion defined in this way

is insensitive to the noise in the original data, due to the averaging effect of the volume computation.

Another operation that we want to study in connection with the erosion is the affine invariant skeletonization of a 3D set [5, 6]. Roughly speaking, the skeleton is a set of points that passes through the “middle” of an object. The computation of skeletons of planar shapes is a subject that received a great deal of attention from the mathematical (see [4, 3] and references therein), computational geometry [17], biological vision [9, 10], and computer vision communities (see for example [14, 19] and references therein). In the classical Euclidean case, the *skeleton* of a planar curve is defined as the set of points equidistant from at least two different points on the given curve, provided the distances are global minima. A number of equivalent definitions exist, and one of them, given by Blum [2, 20], is to define the skeleton points as the shocks on the evolution of the curve which follows the Huygens principle. We define in this paper an analogous skeleton for volumetric sets, the *affine skeleton*, as the shocks of the affine erosion.

In Section 2 we give the basic definitions and we prove basic results about the affine erosion. In Section 3, we describe a numerical procedure to find the affine erosion and to compute an approximation for the skeleton, and in Section 4, we give examples.

2 Definitions and properties

First, we need a definition for the key building block of the affine erosion: the *chord set*. For a convex volume V , the chord set is the volume contained between an oriented plane and the boundary of V , ∂V . However, for a concave volume, we can give several different definitions, depending on how do we treat the crossings between the plane and ∂V . Here we give a definition that later will simplify our numerical computations:

DEFINITION 1: Chord set

Given a bounded set of points $V \subset \mathbf{R}^3$, and a plane Π with normal \mathbf{n} that contains the point $\mathbf{x} \in V$, we define a *chordal sector set* (or for short *chord set*) $\Sigma(\mathbf{x}, \mathbf{n}, V)$, as the **connected** set of points $\mathbf{x}' \in V$ that contain \mathbf{x} and that are in the side of the normal \mathbf{n} of the plane Π , i.e. satisfying $(\mathbf{x} - \mathbf{x}') \cdot \mathbf{n} \leq 0$. We shall denote by $v(\Sigma(\mathbf{x}, \mathbf{n}, V))$ the volume of the chord set.

Like any other volume, the volume of a chordal sector set is invariant under special affine transformations (Eq. 1). This definition implies that any point $\mathbf{x}' \in \Sigma(\mathbf{x}, \mathbf{n}, V)$ is connected to \mathbf{x} by a path $L \subseteq \Sigma(\mathbf{x}, \mathbf{n}, V)$ (see Fig. 1). We can make an interesting hydrostatic analogy: if we slowly inject a liquid in a point P of the surface ∂V , the chord will be the volume of liquid in hydrostatic equilibrium in a

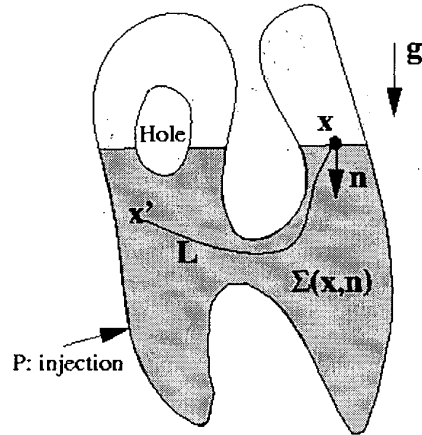


Figure 1. Definition of chord set. In the hydrostatic analogy, the chord $\Sigma(\mathbf{x}, \mathbf{n}, V)$ is the liquid volume injected to the interior of V in hydrostatic equilibrium with a uniform gravity field \mathbf{g} parallel to \mathbf{n} . The point \mathbf{x} is on the free surface of the liquid.

gravity field parallel to \mathbf{n} , and the total volume injected will be $v(\Sigma(\mathbf{x}, \mathbf{n}, V))$ as depicted in Fig. 1.

DEFINITION 2: Erosion level-set function

We define the erosion level-set function $E(\mathbf{x}), V$ as the greatest lower bound of the volume of all chord sets defined by all $\mathbf{x} \in V$,

$$E(\mathbf{x}, V) = \inf_{\mathbf{n} \in S} v(\Sigma(\mathbf{x}, \mathbf{n}, V)) \quad (2)$$

where \inf is computed with the normals \mathbf{n} pointing in all the directions of the unit sphere S . (See Fig. 2.) $E(\mathbf{x}, V)$ is undefined outside the volume.

DEFINITION 3: Erosion-set

The erosion-set Γ_v is defined as the set of points \mathbf{x} satisfying $v \leq E(\mathbf{x}, V)$.

With these definitions, we can prove a few theorems, which are analogous to the two-dimensional case [12, 13].

LEMMA 1: If $V_1 \subseteq V_2$, then $\Sigma(\mathbf{x}, \mathbf{n}, V_1) \subseteq \Sigma(\mathbf{x}, \mathbf{n}, V_2)$.

Proof: If $\mathbf{x}' \in \Sigma(\mathbf{x}, \mathbf{n}, V_1)$ then $(\mathbf{x} - \mathbf{x}') \cdot \mathbf{n} \leq 0$ and it is connected to \mathbf{x} by a connected path $L \subseteq V_1 \subseteq V_2$. Thus, \mathbf{x} is in a connected subset of V_2 that contains \mathbf{x} . From Definition 1, $\mathbf{x}' \in \Sigma(\mathbf{x}, \mathbf{n}, V_2)$. (See Fig. 3) Q.E.D.

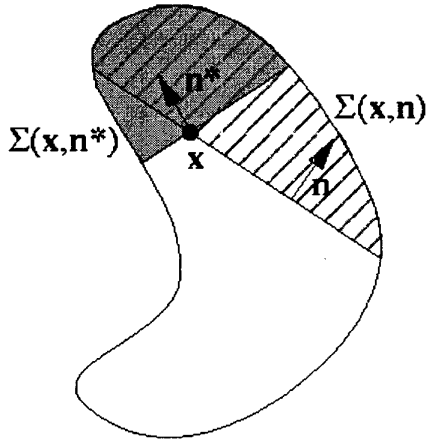


Figure 2. According to the definition, $E(x, V)$ is the volume of the chord $\Sigma(x, n^*, V)$ if for all the other chords $\Sigma(x, n, V)$ the volume is larger or equal than $v(E(x, V))$.

THEOREM 1 [Monotonicity respect to V]: If $V_1 \subseteq V_2$ and $x \in V_1$, then $E(x, V_1) \leq E(x, V_2)$.

Proof: lets consider any point x in the volume V_1 . For any direction n , the chord set satisfies $\Sigma(x, n, V_1) \subseteq \Sigma(x, n, V_2)$ in virtue of Lemma 1. Then,

$$v(\Sigma(x, n, V_1)) \leq v(\Sigma(x, n, V_2))$$

and

$$E(x, V_1) = \inf_{n \in S} (v(\Sigma(x, n, V_1))) \leq$$

$$\inf_{n \in S} (v(\Sigma(x, n, V_2))) = E(x, V_2).$$

Q.E.D.

THEOREM 2 [Inclusion principle]: If $V_1 \subseteq V_2$, then

$$\Gamma_v(V_1) \subseteq \Gamma_v(V_2).$$

Proof: if $x \in \Gamma_v(V_1)$ then $v \leq E(x, V_1)$. From Theorem 1, $v \leq E(x, V_1) \leq E(x, V_2)$, and thus, $x \in \Gamma_v(V_2)$. Q.E.D.

The following theorem will serve to optimize the computation of the erosion set.

THEOREM 3 [Bounds for the erosion level-set function]: $E(x, V)$ satisfies $0 \leq E(x, V) \leq v_0/2$ where v_0

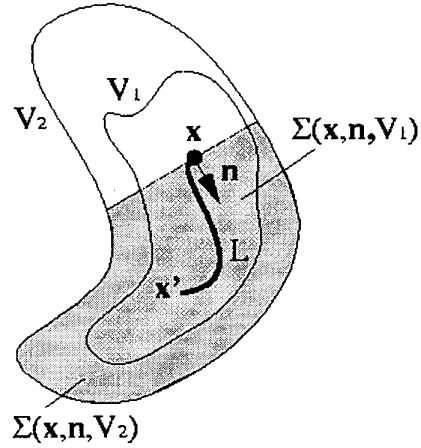


Figure 3. Sketch for Lemma 1.

is the volume of V .

Proof: The two chord sets $\Sigma(x, n, V)$ and $\Sigma(x, -n, V)$ have non-negative volumes $v_1 = v(\Sigma(x, n, V))$ and $v_2 = v(\Sigma(x, -n, V))$, respectively. The volume of the intersection of these chord sets is zero because the intersection is a subset of a plane. As these chords are subsets of V , (see Fig. 4.)

$$v_1 + v_2 \leq v_0.$$

Then, $\min(v_1, v_2) \leq v_0/2$. From Definition 2,

$$E(x, V) = \inf_{n \in S} (v(\Sigma(x, n, V))) = \quad (3)$$

$$\inf_{n \in S} (\min[v(\Sigma(x, n, V)), v(\Sigma(x, -n, V))]) \\ = \inf_{n \in S} (\min(v_1, v_2)) \leq \inf_{n \in S} (v_0/2) = v_0/2$$

Finally, since the volumes of the chord are non-negative, we have from Definition 2, $0 \leq E(x, V)$. Q.E.D.

THEOREM 4 [Monotonicity respect to the chord volume v]: If $v_1 \geq v_2$ then $\Gamma_{v_1} \subseteq \Gamma_{v_2}$. (Here both erosion sets are computed for the same volume V .)

Proof: if $x \in \Gamma_{v_1}$ then $E(x, V) \geq v_1 \geq v_2$, thus, from Definition 3, $x \in \Gamma_{v_2}$. Q.E.D.

The next definition is about a possible use of the 3D affine erosion. We define an skeleton in the analogous way that Blum [2] defined Euclidean skeletons in terms of shocks.

DEFINITION 4: 3D Affine invariant skeleton

We define the *affine skeleton* of V as the set of shocks (or discontinuities on the normals) of the contour surfaces $E(x, V) = \text{const}$ (corners of the erosion-sets).

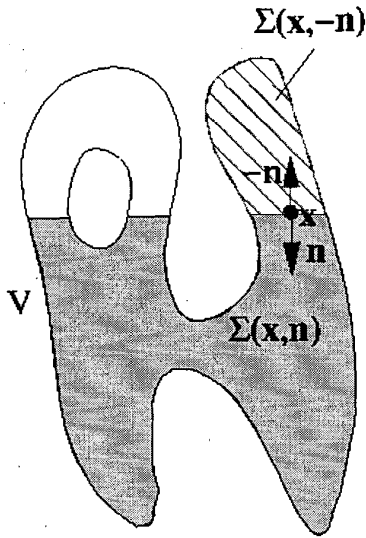


Figure 4. Sketch for Theorem 3.

This definition is consistent with the Euclidean case and makes sense because an affine transformation will preserve shocks.

3 Numerical computation of the affine erosion

In principle, we could use Definition 2 to compute $E(\mathbf{x}, V)$, by computing the volumes of all the chord sets $\Sigma(\mathbf{x}, \mathbf{n}, V)$ and taking the minimum over every normal \mathbf{n} . This approach was used in [1] for the 2D case. However, in the 3D case we have many more possible orientations for the chords and many more points in the volume, which renders this approach computationally infeasible from a practical point of view.

Thus, we propose an alternative algorithm to compute the affine erosion, which is much faster because it takes advantage of the fact that the volume of the chords $\Sigma(\mathbf{x}, \mathbf{n}, V)$ is the same for all the chordal points lying on the plane $(\mathbf{x}' - \mathbf{x}) \cdot \mathbf{n} = 0$. We present the algorithm in a high-level “pseudocode” format.

The input of our algorithm is the surface ∂V enclosing a connected volume V , given implicitly in terms of the level set function

$$\begin{aligned} F(\mathbf{x}) &> 0 && \text{for interior points,} \\ F(\mathbf{x}) &= 0 && \text{for points on the surface,} \\ F(\mathbf{x}) &< 0 && \text{for exterior points.} \end{aligned} \quad (4)$$

This level-set function is discretized in a volumetric array F_{ijk} , $1 \leq i, j, k \leq d$ and $x = i\Delta x$, $y = j\Delta y$, $z = k\Delta z$.

1- Find a triangulation for the surface. We shall denote by T_i , $1 \leq i \leq n$ the individual oriented triangles on the surface. Here we used the marching cubes algorithm to do so [11].

2- Compute the volume v_0 of V . We used a boundary integral formula approximated with the triangles T_i ,

$$v_0 = \frac{1}{3} \oint \mathbf{x} \cdot d\mathbf{S} \approx \frac{1}{3} \sum_{i=1}^n \mathbf{x}_i \cdot \Delta \mathbf{S}_i$$

where $\Delta \mathbf{S}_i$ is the area of the triangle T_i times its normal, and \mathbf{x}_i is its center of mass.

3- For each triangle T_i do

3a- Compute its inwards normal \mathbf{n}_i and its center of mass \mathbf{x}_i .

3b- Define a plane Π^0 with normal \mathbf{n}_i containing \mathbf{x}_i , i.e., $(\mathbf{x} - \mathbf{x}_i) \cdot \mathbf{n}_i = 0$.

do for $l = 1, 2, \dots$:

- Advance the plane a distance $\Delta d = \min(\Delta x, \Delta y, \Delta z)$ in the direction of its normal (towards the interior of the volume). The advanced plane is given by

$$\mathbf{x}_i^l = \mathbf{x}_i + \mathbf{n}_i l \Delta d$$

and

$$\Pi^l \equiv (\mathbf{x} - \mathbf{x}_i^l) \cdot \mathbf{n}_i = 0.$$

- Next, find the connected chordal points \mathbf{x}' by recursively visiting the neighbors of the volume elements that are inside the surface and under the plane, i.e. satisfying

$$F(\mathbf{x}') \geq 0$$

and

$$(\mathbf{x}_i^l - \mathbf{x}') \cdot \mathbf{n}_i \leq 0.$$

For efficiency, just visit the volume elements that are between Π^{l-1} and Π^l . Save the chord set points \mathbf{x}' in a list L . The boundary of this chord set must be carefully triangulated. Here we used again the marching cubes algorithm. Let's call the oriented triangles on the boundary of this region T_k^b , $1 \leq k \leq m$ (the normals of these triangles point towards the interior of the volume). When a triangle lies across the cutting plane Π^l , the triangle must be split accordingly.

- Compute the volume v^l enclosed between the plane Π^l and the surface with a boundary integral:

$$v^l = \frac{1}{3} \oint (\mathbf{x} - \mathbf{x}_i^l) \cdot d\mathbf{S} \approx \frac{1}{3} \sum_{k=1}^m (\mathbf{x}_k - \mathbf{x}_i^l) \cdot \Delta \mathbf{S}_k^b,$$

where $\Delta \mathbf{S}_k^b$ is the area of the triangles T_k^b of the boundary of the chord set times their normal.

end do (3b) until $v^l \geq v_0/2$.

3c- With the values v^l , $l = 1..l_{\max}$, make a linear interpolation $v_{int}(l)$ that represents the volume of a chord defined with a plane at a distance $l\Delta d$ from the 'injection point' \mathbf{x}_i .

3d- Compute $E(\mathbf{x}, V)$: for each one of the chord set points with coordinates \mathbf{x} saved in the list L in step (3), the volume corresponding to a chord $\Sigma(\mathbf{x}, \mathbf{n}_i, V)$ will be $v_{int}((\mathbf{x} - \mathbf{x}_i) \cdot \mathbf{n}_i)$. Compute

$$E(\mathbf{x}, V) := \min(E(\mathbf{x}, V), v_{int}((\mathbf{x} - \mathbf{x}_i) \cdot \mathbf{n}_i)).$$

When computing the minimum, save in a three dimensional vector $\mathbf{N}(\mathbf{x})$ the normal that produces the minimum volume. We shall use this quantity later for computing the skeleton.

4- Repeat (3) until all the triangles of the surface are used.

The method is optimized with the help of Theorem 4, by avoiding the computation of those volumes that are greater than $v_0/2$. Most of the computing time is approximately distributed as follows: computation of the boundaries of the chord sets T_k^b , 33%, search of the connected elements for the chords, 53%, and the computation of the chord volumes, 14%.

The output of this program is a tree dimensional array describing $E(\mathbf{x}, V)$ and another array with the normals $\mathbf{N}(\mathbf{x})$ that define the optimal chords.

Introduction of more cutting planes.

In this algorithm we are dealing with n (= number of triangles) cutting planes. In order to approximate properly the erosion defined by Eq. (2), we should use a very large number of planes. The algorithm described above may have problems with surfaces that have little variety of normals in the surface, like a cube, which will generate just six different planes if we apply the algorithm as described above. In order to introduce a richer distribution on the normals, we can use a *Monte Carlo* technique, where in Step 3 we select a normal at random (i.e. the normalized vector $(n_1, n_2, n_3)/\sqrt{n_1^2 + n_2^2 + n_3^2}$ where each n_i is a pseudo-random number in $(-1, 1)$ with uniform deviate [16]). When the number of triangles on the surface is large enough, the effect of the randomness is not noticeable.

In order to find a numerical approximation for the skeleton, we must look for the shocks in $E(\mathbf{x}, V) = \text{constant}$. This can be accomplished by selecting those points where the absolute value of the mean curvature $\kappa(\mathbf{x})$ of the surfaces $E(\mathbf{x}, V) = \text{constant}$ is greater than a fixed threshold of the order of the inverse of the discretization size,

$$\kappa(\mathbf{x}) = \nabla \cdot \mathbf{N}(\mathbf{x}) \approx \frac{\alpha}{\min(\Delta x, \Delta y, \Delta z)} \quad (5)$$

where α is a number of the order of unity. We compute the divergence with finite differences using the optimal-chord normals \mathbf{N} given by the algorithm in step 3e, and we store the curvatures in a three dimensional array. In order to find the points satisfying Eq. (5) we use marching cubes.

4 Examples

In Fig. 5 we show the erosion of a volume that was generated by elongating and deforming a sphere

$$(3x + 2 \sin \pi z)^2 + (3y + 2 \cos \pi z)^2 + z^2 - 1 = 0.$$

In order to represent this surface we generated a grid of $100 \times 100 \times 100$ points where we evaluate the left hand side of the above expression. In the bottom of Fig. 5 we corrupted the initial shape by adding a random number of uniform deviate to each of the points of the volumetric grid. This example shows the insensitivity of the erosion sets respect to the noise.

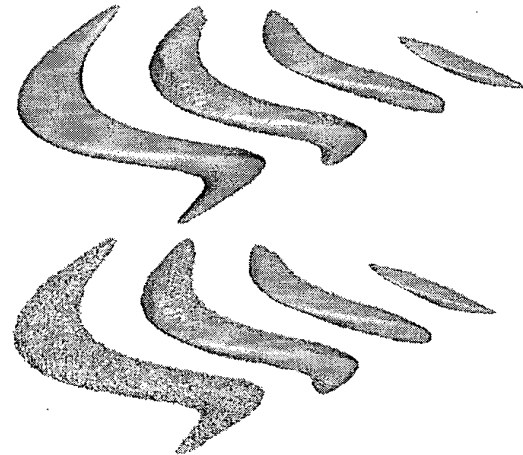


Figure 5. A non-convex volume obtained by elongating and twisting a sphere. The discretized domain has 100 cubed points. Above, without noise, below, with noise. The volumes are $E(\mathbf{x}, V) \approx 0, 1306, 5228, 11772$ and the total volume is 20929.

In Fig. 6 we show the erosion of a cube, and the erosion of the same cube in which we cut a groove on one side. This example illustrates two important properties:

- a) The erosion sets of a simply connected volume may be either connected or not, depending on the initial shape.
- b) The inclusion principle: if the whole cube contains the grooved-cube, then the erosion sets of the first contains the

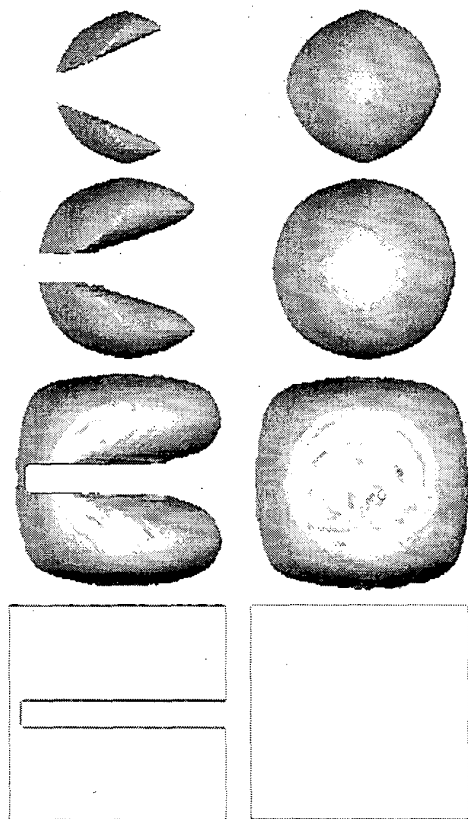


Figure 6. Illustration of the maximum principle and topology change. Left: a cube with a groove, and its erosion for $E(x,V) = 0, 2496, 9986, 17742$ (from bottom to top). Right: the whole cube, and the corresponding erosion for the same volumes.

erosion sets of the second. In Fig. 7 we show the erosion of a shape with a more complex topology. This example also shows clearly that may be topological changes on the affine erosion. We next consider an ellipsoid. First note that according to our definition, the erosion of a sphere is a set of concentric spheres. The only discontinuity on the erosion level set normals is at the center of the sphere, and thus, according to Definition 4, this is its skeleton. We can generate an ellipsoid by making an affine transformation to a sphere, thus, in virtue of the affine invariance, the skeleton of an ellipsoid is its center. In Fig. 8 we show the numerical skeleton of an ellipsoid with noise. The search of good criteria to detect shocks on the affine erosion is still an open problem. Here we are approximate the shock position with the point where the medial curvature is greater in magnitude than a

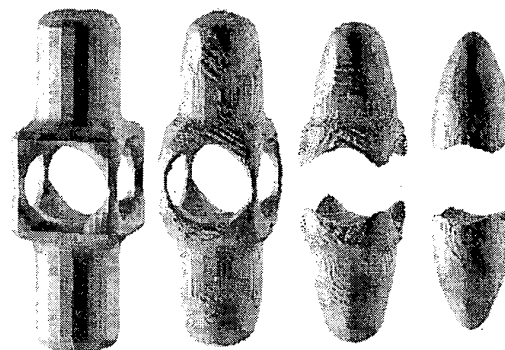


Figure 7. The erosion of a shape with a more complex topology.

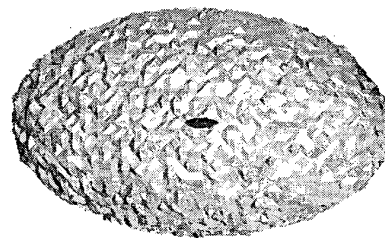


Figure 8. A noisy ellipsoid discretized in a box of 64 points cubed. The skeleton is the black piece in the middle.

given threshold. However, it is still unclear which value has to be used. In order to show how the approximated skeleton depends on this value, in Fig. 9 we show the skeleton of the shape of Fig. 5. Here we computed two approximations for the shocks with $\kappa = 0.75 / \min(\Delta x, \Delta y, \Delta z)$ and $\kappa = 1.5 / \min(\Delta x, \Delta y, \Delta z)$.

5 Conclusion and Further Research

In this paper we discussed a new approach to 3D erosion and 3D skeletonization based on the notion of affine distance. This methodology has significant advantages over the classical Euclidean case since the operations are much more resistant to noise.

However since affine distance is based on areas and volumes (in the 3D case), it is a more global object than the Euclidean distance which makes it slower to compute. We have discussed ways of speeding up the computation. We would like to find faster implementations. The algorithm which we have proposed for affine erosion is $O(N^{5/3})$

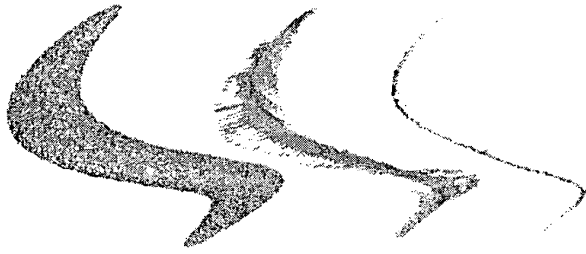


Figure 9. Contour surfaces of the median curvature of the erosion level-set function: From left to right: original surface, $k=0.75$ and $k=1.5$. They may be used as a first approximation for the skeleton.

where N is the number of voxels discretizing the volume, because we are touching every point of the volume as many times as there are triangles on the surface. We are investigating ways of speeding this up.

Another open problem is the definition of more advanced criteria for the detection of shocks on the erosion sets. The fundamental problem here is the reliable detection of a shock for a function discretized in a regular array of real numbers, without confusing the real shocks with discretization effects (see [20] for a related work on the context of euclidean skeletons).

References

- [1] S. Betelu, G. Sapiro, G., A. Tannenbaum, and P. Giblin, "Noise resistant affine skeletons of planar curves", *ECCV2000*, Dublin, June 2000.
- [2] H. Blum, "Biological shape and visual science," *J. Theor. Biology* **38**, pp. 205-287, 1973.
- [3] J. W. Bruce and P. J. Giblin, *Curves and Singularities*, Cambridge University Press, Cambridge, 1984; second edition 1992.
- [4] J. W. Bruce, P. J. Giblin and C. G. Gibson, "Symmetry sets," *Proc. Royal Soc. Edinburgh* **101A** pp. 163-186, 1985.
- [5] P. Giblin and G. Sapiro "Affine invariant symmetry sets and skew symmetry," *International Conference on Computer Vision*, Bombay, India, January 1998.
- [6] P. J. Giblin and G. Sapiro, "Affine invariant distances, envelopes and symmetry sets", *Geom. Ded.* **71**, pp. 237-261, 1998.
- [7] H. Heijmans, "Mathematical Morphology: Basic principles", *Proceedings of Summer School on Morphological Image and Signal Processing*, 1995, Zakopane, Poland
- [8] A. K. Jain, *Fundamentals of digital Image Processing*, Prentice Hall Information and system sciences series, 1989.
- [9] I. Kovács and B. Julesz, "Perceptual sensitivity maps within globally defined visual shapes," *Nature* **370** pp. 644-646, 1994.
- [10] M. Leyton, *Symmetry, Causality, Mind*, MIT-Press, Cambridge, 1992.
- [11] K. Martin, W. Schroeder, B. Lorensen, *The Visualization Toolkit An Object-Oriented Approach To 3D Graphics*, Prentice Hall 1999.
- [12] L. Moisan, "Affine Plane Curve Evolution: A fully consistent scheme," *IEEE Transactions on Image Processing*, **7**, pp. 411-420, (1998)
- [13] L. Moisan, *Traitement numerique d'images et de films: equations aux derivees partielles preservant forme et relief*, Ph.D. Thesis, Universite Paris IX Dauphine U.F.R. Mathematiques de la Decision.
- [14] R. L. Ogniewicz, *Discrete Voronoi skeletons*, Hartung-Gorre Verlag Konstanz, Zurich, 1993.
- [15] R. Owens, *Dilation/Erosion*, CV-Online, 2000.
- [16] W. Press, S. Teukolsky, W. Vetterling, and Flann, *Numerical Recipes: The Art of Scientific Computing*, Cambridge University Press, (1992).
- [17] F. P. Preparata and M. I. Shamos, *Computational Geometry*, Texts and Monographs in Computer Science, Springer-Verlag, New York, 1990.
- [18] I. Ragnemalm, "Fast erosion and dilation by contour processing and thresholding of distance maps", *Pattern Recognition Letters* **13** pp.161-166, (1992)
- [19] J. Serra, *Image Analysis and Mathematical Morphology*, Vol. 1, Academic Press, New York, 1982.
- [20] K. Siddiqi, S. Bouix, A. Tannenbaum, and S. W. Zucker., "The Hamilton-Jacobi skeleton," *ICCV'99*, pages 828-834, Kerkira, Greece, September 1999.